CONF - 810602--25

LA-UR -81-1067

TITLE: DETONATION PRESSURES OF PBX-9404, COMPOSITION B, PBX-9502, AND NITROMETHANE

MASTER

AUTHOR(S): W. C. Davis and J. B. Ramsay

SUBMITTED TO: Seventh Symposium on Detonation
Naval Surface Weapons Center

DISCLAIMER

University of California

LOS ALAMOS SCIENTIFIC LABORATORY
Post Office Box 1663 Los Alamos, New Mexico 87545
An Affirmative Action/Equal Opportunity Employer

Form No. 836 R3
St. No. 2629

UNITED STATES
DEPARTMENT OF ENERGY
CONTRACT W-7405-ENG. 36

DETONATION PRESSURES OF PBX-9404, COMPOSITION B, PBX-9502, AND NITROMETHANE

W. C. Davis and J. B. Ramsay
Los Alamos National Laboratory
Los Alamos New Mexico

Measurements of detonation pressure for PBX-9404, Composition B, PBX-9502, and nitromethane are presented. The interpretations of the data are discussed, and the implications are compared with results from other experiments. The pressures are considered from the point of view of their use as calibrations for calculations, and suggestions are given for slight changes from the measured value for use with limited calculation procedures.

INTRODUCTION

Data from a number of different types of experiments are presented and evaluated, to obtain estimates of the detonation pressures of the explosives PBX-9404, Composition B, PBX-9502, and nitromethane. The desired pressure is that at the end of the reaction zone in a steady plane detonation, i.e., the Chapman-Jouquet pressure. The results are summarized in Table I.

TABLE I
Summary of Detonation Pressures and Related Data

Explosive	Density g/cm^3	Pressure GPa	Wave Velocity m/s	γ_j
PBX-9404	1.846	35.6±0.4	8.776	2.99
Composition B	1.730	26.3±0.4	7.95	3.16
PBX-9502	1.895	28.9±1	7.706	2.89
Nitromethane	1.133 (23C)	13.4±0.4	6.299	2.36

Interpretation of experimental data is never independent of the model used. Even a curve through the data points implies a model, or at least restrictions on a model. Figure 1 shows a diagram of the pressure profile for the ZND model of steady detonation. The leading front is a shock wave that compresses and heats the explosive to start the chemical reaction. The region where the reaction takes place is called the reaction zone, as marked on the diagram. When the reaction is finished, expansion continues in a nonsteady flow region. When the nonsteady flow is one-dimensional and self-similar, the expansion region is called the Taylor wave. The model is strictly applicable only to plane, laminar flow, with the reaction zone a steady flow region (i.e., the reaction zone is independent of time in a coordinate system attached to the plane shock wave). The model then treats only detonations that propagate with constant velocity and constant pressure profile in the reaction zone. If the reaction zone is negligibly thin compared with the size of the explosive charge, a simpler model called the CJ model of detonation is often used. The reaction zone in Fig. 1 shrinks to nothing; the only part of it that remains is the point that marks the end. This point, called the CJ point, is the initial state for the following expansion. Most computer codes for hydrodynamic calculations of systems using explosives are based on this simple model. It is very difficult to treat the reaction zone properly in a code, in part because the ZND model has two time scales. A very short one is

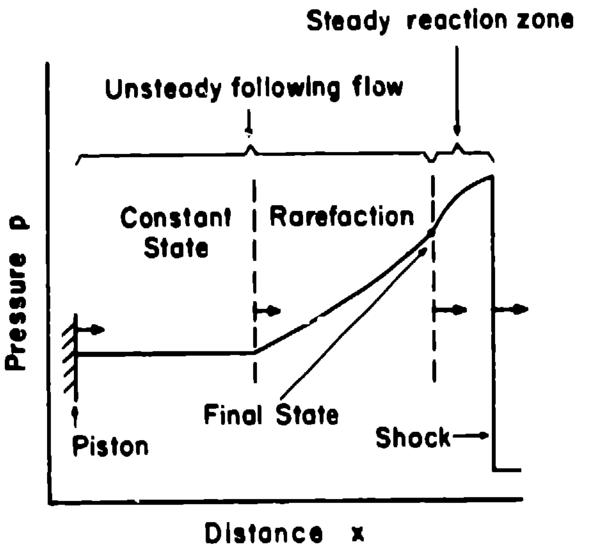

Fig. 1. ZND Model of a steady plane detonation reaction zone.

needed for the reaction zone, and most of the reaction takes place in a small part of the zone, so very fine cells are required to get enough accuracy for good simulation. A much longer time scale is needed for the rest of the problem, which is the interaction of the expanding detonation gases with the driven metal parts. Coarser cells can be used for this portion. If fine cells are used throughout both regions, the problem becomes prohibitively slow and expensive because of the unnecessary detail.

The important calibration point for either model is the CJ pressure. For the ZND model, we define the CJ pressure to be the pressure at the end of the reaction zone where the unsteady expansion attaches to the steady reaction zone. If the real system has an appreciable reaction zone, but is to be modeled using the CJ code, it may be necessary to adjust the CJ pressure upward a little to account for the extra pressure and momentum in the reaction zone. If so, the "calibration" changes with the size of the system.

From the ZND model, we see that every explosive has a length and time scale of its own, determined by the length and time for the reaction to be completed. In practical arrangements, the reaction zone will not be set up in its steady form by the initiating system, and the steady state will be approached asymptotically after the transient behavior. Every explosive is expected to have transients; the important question is whether they cause an appreciable effect in the systems that interest us. The ratio of reaction zone length to some length characteristic of the system determines the importance of the transient effect. For a particular system size, one explosive might have negligible transient effect, while another, with a longer reaction zone, might have a large effect.

Some work has been done to extend [1,2] the ZND model to detonation that is slightly nonsteady, and calculations with resolved reaction zones have been made. The details will not be discussed here. Instead, we look at the experimental data to see whether transients are important in PBX-9404 and Composition B.

The discovery, many years ago, that the detonation velocity for an explosive composition is a constant value characteristic of the material, led to the postulate of a steady reaction zone that underlies the theory. Reversing the argument, we expect the detonation velocity to be different from the steady value if the reaction zone is not steady. By measuring detonation velocity for different charge lengths, the distance over which the initiation transient has appreciable effect can be determined. Figure 2 shows measurements [3] of detonation velocity vs charge length for PBX-9404 and Composition B. The dashed lines are the constant detonation velocities characteristic of these materials. Within the small scatter of the measurements, the velocity for PBX-9404 is constant at the steady value. The transient is unimportant, at least after the

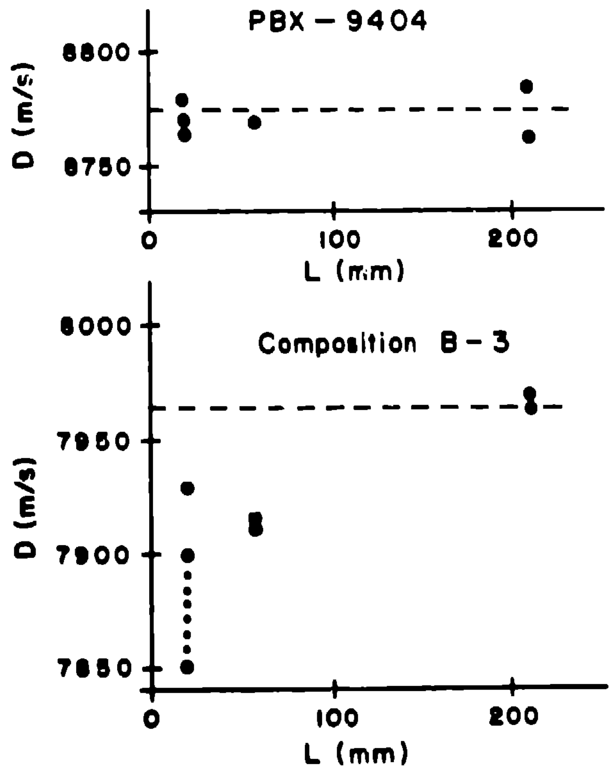

Fig. 2. Detonation velocity vs charge length for PBX-9404 and Composition B. The dashed line shows the steady detonation velocity.

wave has run 15 or 20 mm. For Composition B, on the other hand, the velocity is well below the steady value even after more than 50 mm of travel, and we can expect to find effects of the initiation transient in large charges.

The reaction zone length and shape, besides setting the scale for the transient, set the scale for edge effects. We cannot infer any detailed relationship, but we expect that if one explosive shows a slower decay of the initiation transient than another, it will also show edge effects at larger diameter than the other does. Figure 3, from the work of Campbell

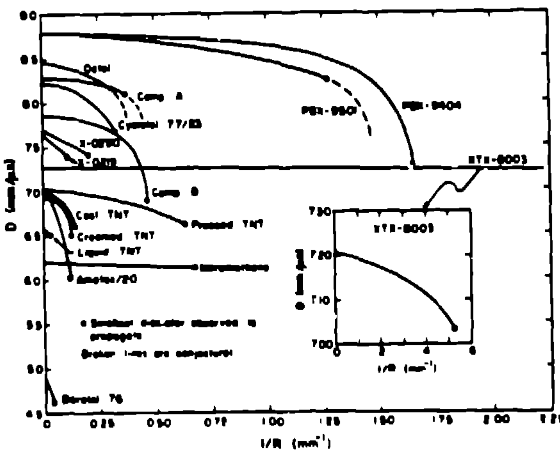

Fig. 3. Detonation velocity vs reciprocal charge diameter for a number of explosives. The new designation for X-0290 is PBX-9502.

and Engelke [4], shows detonation velocity plotted against reciprocal radius for a large number of explosives, among them PBX-9404, Composition B, PBX-9502, and nitromethane. Although the graph shows curves of different shapes for different explosives, the curves for PBX-9404 and Composition B are quite similar. Table II shows a comparison of the fit parameters found by Campbell and Engelke. Their ratio for Composition B and PBX-9404 is between three and four, which means that the scale for edge effects is three or four times larger for Composition B than for PBX-9404. Since the reaction zone is sampled differently by the transient effect and the diameter effect, we can draw no conclusion except that the two explosives are ordered the same way.

Magnetic probe measurements are made by embedding a plane metal foil in the flow system, arranging a divergent magnetic field through it, and placing a pickup coil outside the flow system. When the flow moves the foil, eddy currents are induced in it. These currents change the field at the coil and induce a voltage. The analysis, simple in principle but lengthy, relates the foil velocity to the observed voltage. The data, then, are in the form of a continuous record of particle velocity of the foil at a function of time.

Magnetic probe measurements for PBX-9404, Composition B, and PBX-9502 were presented by Davis [5]. Results are shown in Figs. 4, 5, and 6. The data in Fig. 4, for PBX-9404, are for five different charge lengths. There is no evidence of a reaction-zone spike at the front as in Fig. 1. The dashed lines are particle velocities, found from a calculation for an identical system, describing the explosive with a CJ model with infinitesimal reaction zone and a CJ pressure of 35.6 GPa. The fit is adequate within the two-percent accuracy of the measurements. The data for the shortest charge length are a little low at the front, and perhaps a little too flat to agree with the calculation. Possibly the transient is responsible for the difference, but the data are not good enough to tell. At any rate, the effect is small or absent and certainly no large transient effects are present.

The data for Composition B, Fig. 5, show a reaction-zone spike that has an appreciable effect out to about 1/2 μs, in agreement with the detonation velocity results. The pressure at the end of the reaction zone is not constant, but varies with the length of the charge. However, a calculation using a CJ model, shown by the dashed lines, seems to be a reasonable fit to the data after the reaction is over. The pressure for the calculations is 27.4 GPa. The

TABLE II
Diameter Effect Parameters

$$D(r) = D(\infty)\,[1 - A/(r - r_c)]; \quad r_f = \text{failure radius}$$

	A μm	A/A_1	r_f μm	r_f/r_{f1}
PBX-9404	890	1	590	1
Composition B	2840	3.19	2140	3.63
Nitromethane	2600	2.92	1420	2.41
PBX-9502	19400	21.8	4500	7.63

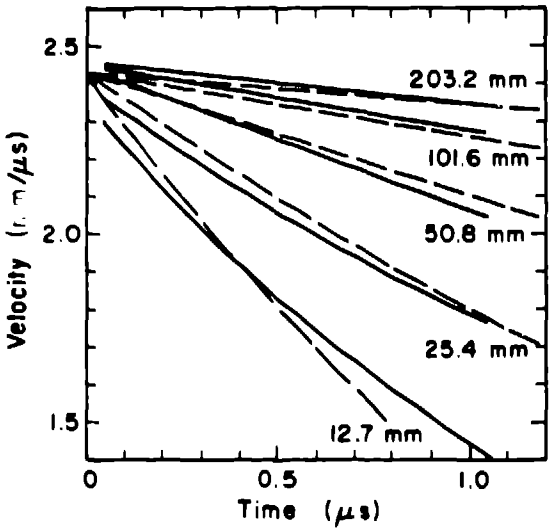

Fig. 4. Magnetic probe measurements of particle velocity in a plane detonation system using PBX-9404. The numbers on the curves are the charge lengths. The dashed lines are calculations of the motion made using a CJ model with CJ pressure 35.6 GPa.

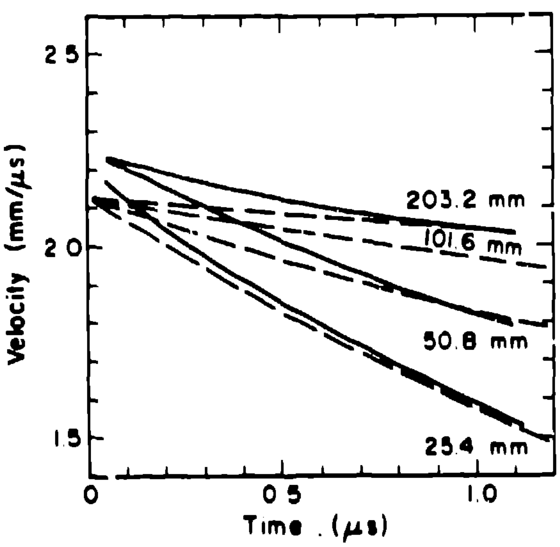

Fig. 5. Magnetic probe measurements of particle velocity in a plane detonation system using Composition B. The numbers on the curves are the charge lengths. The dashed lines are calculations of the motion made using a CJ model with CJ pressure 27.4 GPa.

free-surface velocity measurements discussed below give 26.3 GPa for the real CJ pressure at the end of the reaction zone. In our discussion above of the calibration of a CJ Model to be used for an explosive with a resolvable reaction zone, it was pointed out that the apparent

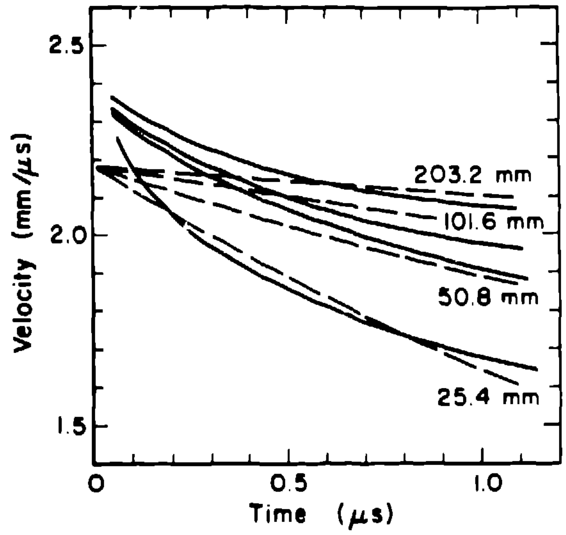

Fig. 6. Magnetic probe measurements of particle velocity in a plane detonation system using PBX-9502. The numbers on the curves are the charge lengths. The dashed lines are calculations of the motion made using a CJ model with CJ pressure 29.3 GPa.

pressure might have to be adjusted upward a little to make it work, and here we have an example.

The data for PBX-9502, Fig. 6, show a reaction zone spike larger than that for Composition B, and lasting a little longer. Again, the pressure at the end of the reaction zone varies with the length of the charge. A calculation using a CJ model with pressure 29.3 GPa is a reasonable fit to the data after the reaction is over. The extra momentum in the reaction zone will drive inert parts with more energy than the calculation suggests, and an even higher pressure is needed for simple computations.

In 1945 Goranson suggested that explosive pressures could be inferred from measurements of the free-surface velocities of metal plates driven by a plane detonation wave. By firing a series of experiments with the same metal, but with a range of plate thicknesses, the shape of the reaction zone and expansion wave (see Fig. 1) can be mapped out. Furthermore, by firing additional series with a different metal, the reflected shock Hugoniot curve and the expansion isentrope curve can be mapped out, too. An enormous number of shots has been fired to make all these measurements.

The results for Composition B have been published [1,6-8] and interpreted several times. The initial interpretation was, of course, in terms of the CJ model; the latest and best [1] uses a sophisticated nonsteady model to fit all the measurements, not only of free-surface velocity, but diverse others. The detonation velocity data of Fig. 2 are in agreement with this model. The detonation wave looks, at any chosen instant, much like the ZND model shown in Fig. 1, with the reaction zone 1/2 μs long, and the CJ pressure 26.3 GPa. However, the reaction zone profile changes with the length of the charge. Although the measured points near the front of the reaction zone increase about 10 percent over the range of lengths used for experiments, the measured pressure at the true end of the reaction (the point that becomes the CJ point in the limit of infinite run), increases less than one percent, and the slope of the "Taylor wave" is hardly distinguishable from that found for a CJ model. The only obvious effect of the buildup with length is within the reaction zone.

Some of the Composition B data from free-surface velocity measurements are shown in Fig. 7. They give a very confused idea of initial free-surface velocity, apparently changing with charge size. The two-reaction model, with only a very small fraction (about four percent) of the total energy liberated in the slow reaction, fits all the data very well. Examples of the fit are shown in Figs. 8 and 9; the fits [1] to the rest of the data points are also good. The time-dependent change is almost entirely within the reaction zone, and later

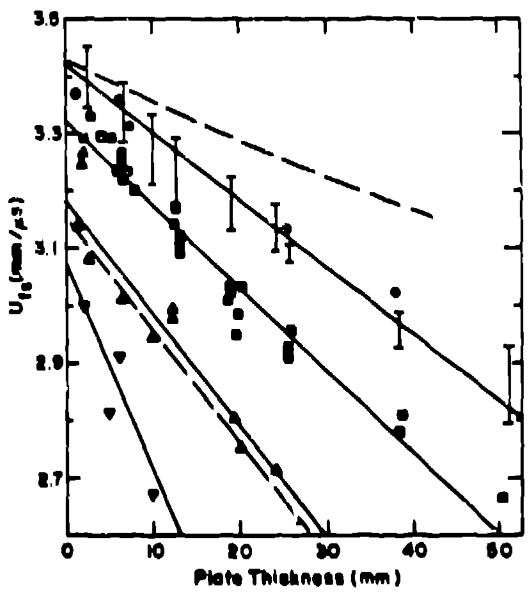

Fig. 7. Free-surface velocity vs plate thickness data for a one-dimensional Composition B/dural system. The charge lengths are 203.2 mm (●), 101.6 mm (■), 50.8 mm (▲), and 25.4 mm (▼). The dashed lines are the result of calculations made using γ-law equations of state for the explosive gases and a Mie-Gruneisen equation of state for the dural. They correspond to CJ pressures of 26.8 and 29.3 GPa.

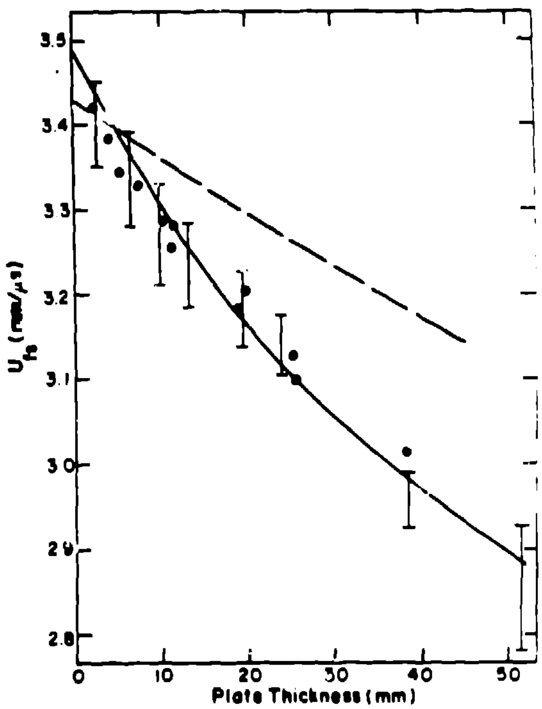

Fig. 8. The free-surface velocity of dural plates induced by a 203-mm charge of Composition B. The solid line is calculated from the model; the dashed lines is for a CJ model with p_j = 29.3 GPa.

expansion is nearly unaffected. The measurement technique exaggerates the effect, because it samples the Taylor wave only very close to the front.

Free-surface velocity data for PBX-9404, although extensive, have not been published, and the experiments themselves are not satisfactorily described and discussed. Some interpretation [9] was done. Apparently, the reason for this near absence of publications arose because the first set of measurements was classified when PBX-9404 was new, and workers have failed to publish, rather than face the problems of relating their new data to older classified data. Figure 10 shows our collection of the measured points, for free-surface velocity of dural plates driven by a plane wave detonation in PBX-9404. The curves in Fig. 10 are calculated free-surface velocities using the PAD code; a CJ model and a constant-γ equation of state for the explosive; and an elastic, perfectly plastic model for the dural, with yield strength 0.3 GPa and shear modulus 25 GPa. Most of the data are fit pretty well with this model for a CJ pressure equal to 35.6 GPa. The points for one-inch charge length might be better fit by 34.5 GPa, and the ones for one-half inch length by 32.5 GPa. The detonation velocity data shown in Fig. 2 do not support this apparent observation of pressure

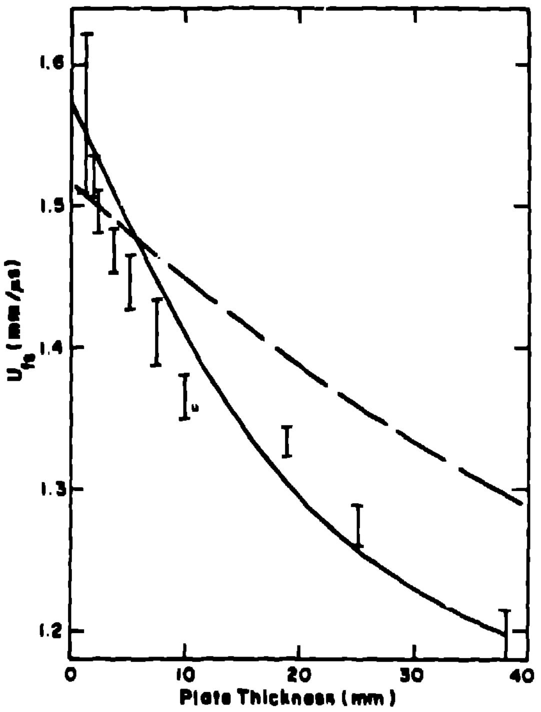

Fig. 9. The free-surface velocities induced into uranium by 203 mm of Composition B. The solid line is calculated from the model; the dashed line is for a CJ model with p_J = 29.3 GPa.

buildup, but the magnetic probe data in Fig. 5 could be taken to suggest it. An alternate explanation might be that strain-rate dependent strength of the dural must be taken into account. The discrepancy remains to be explained. Even so, the pressure at one-inch length is down only three percent if the data are fit with the simple model used here, and at one-half inch the effect is less than nine percent. The buildup model used to treat the data for Composition B, discussed above, showed that although the reaction zone profile changed a lot, the Taylor wave changed very little. At present we cannot understand how PBX-9404 could behave very differently.

Nitromethane has been used for many experiments, but the data used to determine its CJ pressure have not been published in any detail. There is not space for them all here, but they can be briefly reviewed. The detonation velocity results in Table II make us think that the reaction zone is almost as long as that of Composition B, but the pressure measurements seem to show no reaction zone effects. Bdzil [10] has estimated that the reaction zone for nitromethane is about 0.07 mm long, as compared with his estimate for PBX-9404 of 0.02 mm. His work uses a new model of detonation in a cylinder. The new theory has not yet been applied to Composition B.

There are several sets of free-surface velocity data for nitromethane. One set of plane-wave measurements is shown in Fig. 11. These seem to follow the computed Taylor wave shape, and show no evidence of any appreciable reaction

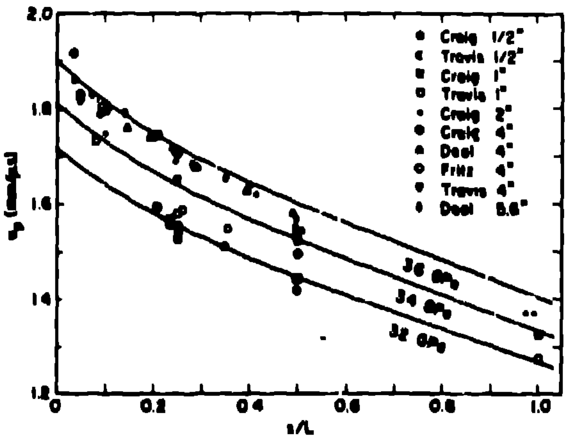

Fig. 10. Particle velocity in dural driven by PBX-9404, inferred from free-surface velocity measurements, plotted vs the ratio of dural thickness to explosive thickness. The lines are calculated velocities for three different CJ pressures using a CJ model for the explosive, and an elastic, perfectly plastic model for the dural.

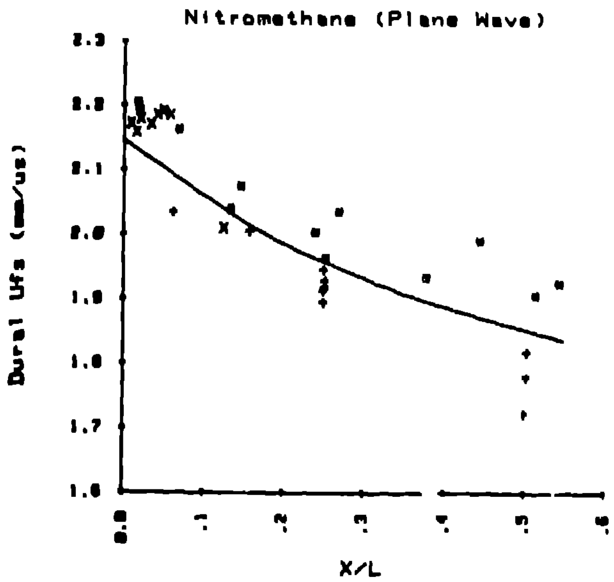

Fig. 11. Plot of some of the free-surface velocity data for nitromethane in the scaled plane. The line is from a CJ model calculation with p_J = 13.4 GPa. There is no evidence of any reaction-zone effects.

zone. Many experiments have also been done where free-surface velocity was measured using long cylinders of nitromethane. One set of these is shown in Fig. 12, plotted against the

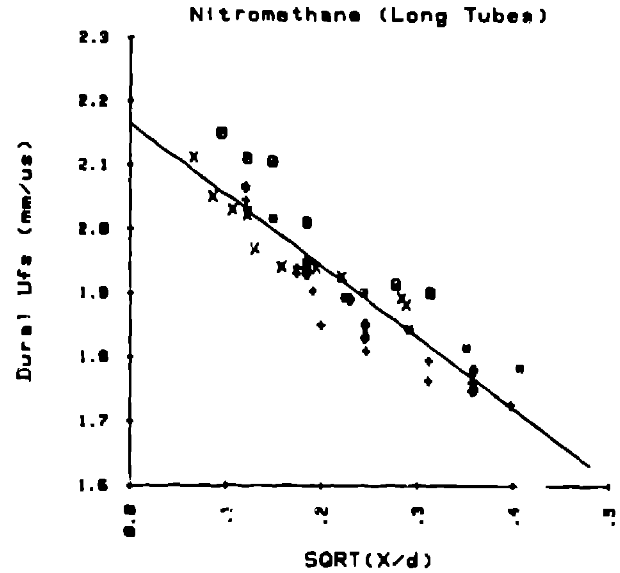

Fig. 12. Plot of some of the free-surface velocity data for nitromethane. These measurements were made using cylindrical charges, and are plotted in a scaled plane to agree with Taylor's treatment of the flow behind a curved sonic surface. The line is a least-squares fit to the points.

square root of the ratio of plate thickness to charge diameter. This scaling is chosen because the sonic surface curved in a cylindrical charge, and Taylor [11] has shown that the inert flow following a curved sonic surface has this form. The results from six different sets of measurements are plotted in Fig. 13. The interpretation of these data is given in the figure caption. The best estimate for the CJ pressure is 13.4 ± 0.4 GPa, for commercial nitromethane (97.5 percent nitromethane, with nitroethane the main impurity) at 23°C.

The free-surface velocity data for PBX-9502 are not nearly as extensive as they are for the other explosives discussed here. Figure 14 shows the data obtained for charges which are 12.7, 25.4, and 50.8 mm long by 108 mm in diam. The results were obtained using the reflected-wire techniques used for many of the other free-surface velocity measurements reported here. All charges were from the same production lot. The average density was 1.895 g/cm^3. The diameter-effect data in Table II and the magnetic probe data lead us to expect behavior with a reaction zone effect comparable to that for Composition B.

The steady-state, infinite diameter detonation velocity of PBX-9502 is 7.706 mm/us. Using

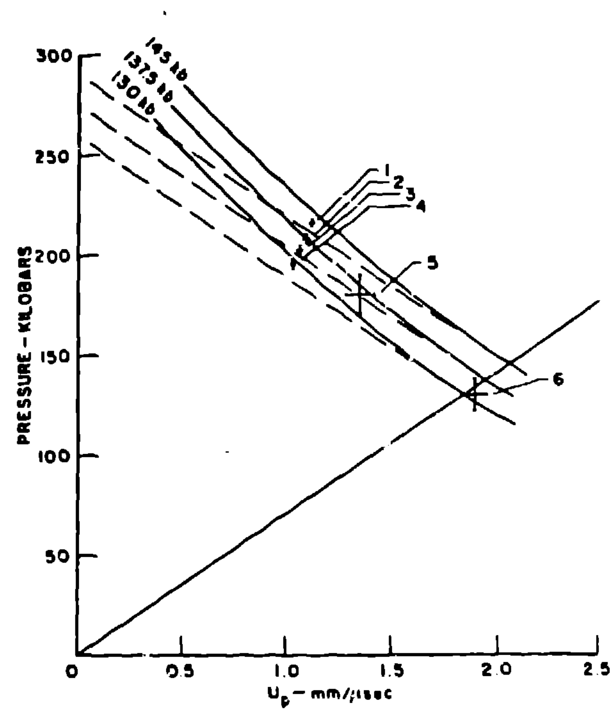

Fig. 13. Plot of the results from six sets of measurements of the initial free-surface velocity for nitromethane. Point 1 is a cylindrical-charge set of data taken at 0°C, and lies about 7 kbar high because of the high density at that temperature. Point 2 is from the plane-wave data of Fig. 11, at 23°C. Point 3 is for the cylindrical-charge data of Fig. 12, at 23°C. Point 4 is for an atypical batch of nitromethane (96 percent NM), for plane-wave charges at 23°C. All these data are for dural plates. Point 5 is for cylindrical charges with glass plates, and point 6 is for cylindrical charges with plastic plates (Sierracin 611), both at 23°C. The straight line is the Rayleigh line for nitromethane.

a velocity deficit of 0.056 mm/us, γ = 2.89, and reserving 1.5 percent of the energy for the second reaction, a two-reaction model was fit to the data obtained for the 25.4-mm-long charges. The corresponding curve for the 12.7-mm-long charges lies below the data, and is above the data for the 50.8-mm-long charges. The computed curves are shown in Fig. 14 with the respective data. A comparison of the two-reaction model using the same parameters to the magnetic probe data is shown in Fig. 15. A small systematic deviation is noted, but the overall agreement is good. The variations during the early part of the computed curve arise from numerical noise. From this analysis, we conclude that the C-J pressure for PBX-9502 (with an initial density of 1.895 g/cm^3) is 28.9 ± 1 GPa.

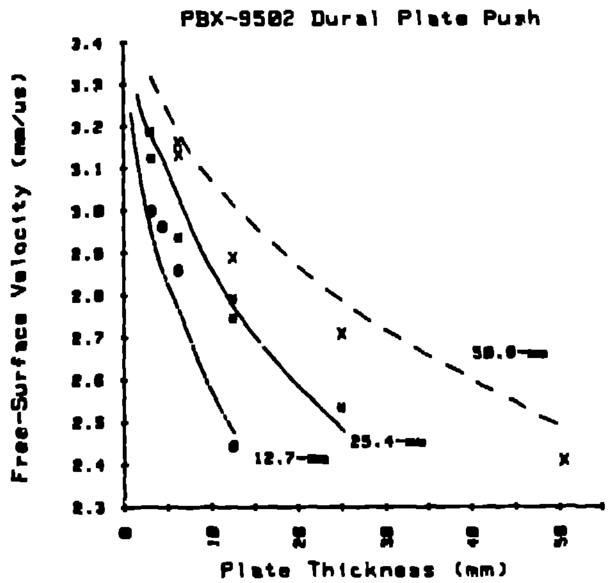

Fig. 14. Free-surface velocity vs dural plate thickness. The points represent the average of three measurements on each shot. The curves were computed using the two-reaction model with $\gamma = 2.89$, 1.5 percent of the energy reserved, and a 0.056 mm/μs initial velocity deficit.

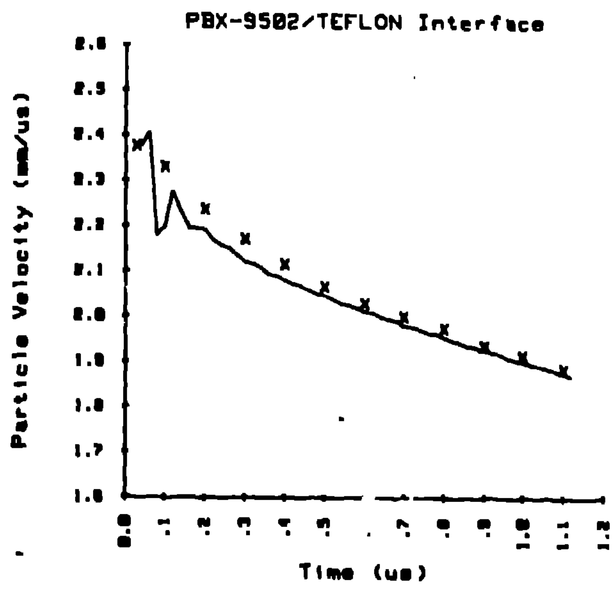

Fig. 15. Magnetic probe data compared with two-reaction model. The x's are averages of two magnetic-probe records for 50.8-mm-long PBX-9502. The curve was computed using the two-reaction model with the same parameter as used for the curves in Fig. 14.

REFERENCES

1. J. B. Bdzil and W. C. Davis, "Time-Dependent Detonations," Los Alamos Scientific Laboratory report LA-5926-MS (1975).

2. J. B. Bdzil, "Perturation Methods Applied to Problems in Detonation Physics," Sixth Symposium (International) on Detonation, Office of Naval Research, ACR-221, 1976, p. 352.

3. W. C. Davis, Detonation Velocity Transient of Composition B-3 and PBX-9404, Phys. Fluids 22, 1407 (1979).

4. A. W. Campbell and Ray Engelke, "The Diameter Effect in High-Density Heterogeneous Explosives," Sixth Symposium (International) on Detonation, Office of Naval Research, ACR-221, 1976, p. 642.

5. W. C. Davis, "Magnetic Probe Measurements of Particle Velocity Profiles," Sixth Symposium (International) on Detonation, Office of Naval Research, ACR-221, 1976, p. 637.

6. W. E. Deal, J. Chem. Phys. 27, 796 (1957).

7. W. E. Deal, Phys. Fluids 1, 523 (1958).

8. W. C. Davis and Douglas Venable, Pressure Measurements for Composition B-3, Fifth Symposium (International) on Detonation, Office of Naval Research, ACR-184, 1970, p. 13.

9. C. L. Mader and B. G. Craig, Nonsteady-state Detonations in One-dimensional Plane, Diverging, and Converging Geometries, Los Alamos Report LA-5865 (1975).

10. J. B. Bdzil, "Steady-State Two-Dimensional Detonation," J. Fluid Mech., to be published June 1981.

11. R. Courant and K. O. Friedrichs, "Supersonic Flow and Shock Waves," Interscience Publishers, New York, 1948, p. 429.